Modeling and Analysis

GREENHOUSE GASES SCIENCE AND TECHNOLOGY

Tracking leakage from a natural CO_2 reservoir (Montmiral, France) through the chemistry and isotope signatures of shallow groundwater

Julie Lions, BRGM, Orleans, France
Pauline Humez, BRGM, Orleans, France and University of Calgary, Canada.
Hélène Pauwels, Wolfram Kloppmann, and Isabelle Czernichowski-Lauriol, BRGM, Orleans, France

Abstract: Natural accumulations and releases of CO_2 provide the opportunity to study the CO_2 trapping and migration mechanisms, the potential impacts of CO_2 leaks, and the monitoring tools to assess the impacts of geological storage of anthropogenic CO_2. Previous studies on the deep CO_2 reservoir of Montmiral (France), focusing on soil gases, groundwater, as well as deep fluids, did not detect any signs of leaks and despite high CO_2 fluxes suspiciously high $\delta^{13}C$ values have not been stated. In order to further investigate whether some CO_2 has leaked from the reservoir toward the surface, we focus here on the major and trace element geochemistry of the shallow aquifers overlying the reservoir with a special focus on the carbonate system, using isotope tracers potentially sensitive to leaks ($\delta^{13}C$ of DIC, $^{87}Sr/^{86}Sr$ and stable isotopes of water). A forward modeling of the potential evolution of groundwater in case of leaks was performed, combining equilibrium calculations of the carbonate system and an *ad hoc* carbon isotope model. Most observed $\delta^{13}C$ values are compatible with modeled carbonate dissolution under open or closed conditions with respect to CO_2. A ^{13}C-enriched subset of samples shows clear signs of incongruent dissolution of Mg-Sr-calcite or dolomite, corroborated by $^{87}Sr/^{86}Sr$ ratios, so that mixing with isotopically heavy deep CO_2 is not required to explain the observed chemical and isotope data. The absence of any sign of CO_2 leakage into shallow groundwater would support the fact that the reservoir and caprock have been trapping the CO_2 efficiently over millions of years.

Keywords: CO_2; fresh groundwater; isotope; leakage; natural analog

Introduction

Leakage of CO_2 in supercritical or gaseous form from onshore or near-shore deep saline aquifers used for geological storage or migration of the associated brines is frequently cited as a risk for the overlying or neighboring shallower potable groundwater resources.[1,2]

The objective of the regulators is to ensure that the geological storage of CO_2 will be permanent and safe

Correspondence to: Dr Julie Lions, BRGM – D3E - Water Environment & Ecotechnologies Division 3 avenue Claude Guillemin, BP 6009, 45060 ORLEANS Cedex 2, France. Email: j.lions@brgm.fr
Received July 29, 2013; revised September 16, 2013; accepted September 16, 2013
Published online at Wiley Online Library (wileyonlinelibrary.com). DOI: 10.1002/ghg.1381

for the environment and human health. Therefore, the storage site selection stage is crucial in order to guarantee that the stored CO_2 will be perfectly and permanently confined.

To date, the geochemical impact of CO_2 storage has mainly been studied at near-well and reservoir scale[3–8] whereas risks in the larger context of regional groundwater systems have not yet been widely assessed.[9,10] There are several CO_2 injection and storage sites where the formation water is monitored, notably for ^{18}O and ^{13}C isotopic ratios.[11–15] Natural CO_2 accumulations, which are common around the world,[16] provide a unique opportunity to study long-term processes that may occur following geological storage of anthropogenic CO_2, and are useful for assessing the impact on water quality in overlying aquifers.

Most natural CO_2 fluxes stem from volcanic activity or from sources such as the degassing of the upper mantle, the decomposition of carbonate rock, or from hydrocarbon reservoirs.[17] In terms of quantity, the principal emission process is the degassing of magma by volcanic activity.[18] Natural CO_2 fluxes in the subsurface can, to a certain extent, be considered as natural analogues of CO_2 geological storage leakage and be used to assess its environmental consequences.[16,19,20] There are also many natural CO_2 traps in sedimentary basins or in volcanic zones (active or dormant) that show that CO_2 can be stored in suitable geological structures for thousands to millions of years due to the presence of efficient cap rocks.[21] Yet, many natural reservoirs are affected by natural upward migration that, in some cases, reaches shallow aquifers.[16]

The Florina Basin (Greece) contains a shallow CO_2 reservoir with gas that reaches the surface and gives rise to carbonate-rich springs. Beaubien *et al.*[22] concluded that the water there has a higher mineralization, which might impair its quality, but no impact on trace elements was demonstrated. In the San Vittorino Basin (Italy), the concentrations of trace elements remain below the drinking-water limits.[22] Main drawback of the study of natural analogues is the fact that the hydrochemical baseline before interaction with CO_2 is unknown, given the long timeframe of natural leakage. Moreover, the long-term leaching of sediments/rocks exposed to CO_2 fluxes may have progressively removed the potentially toxic trace elements (i.e. heavy metals) from the aquifer material so that they cannot be identified anymore in present-day groundwater.

In France, such natural analogues were encountered in the French South-East Basin and this paper focuses on the CO_2 reservoir of Montmiral.[19,23,24] This natural accumulation of CO_2 (97 to 99% of the gas phase) takes the form of a CO_2-rich brine located between 2300 and 2500 m depth. Above the reservoir, close to the surface, there are two main shallow aquifers: one is local and superficial (alluvial), the other is a regional multilayered aquifer (Miocene molassic formation) with old groundwater in depth. In these aquifers, around 30 wells are accessible and detailed analyses were performed on groundwater (major ions, metals, REE, $\delta^{18}O$, $\delta^{2}H$, $\delta^{13}C$, $^{87}Sr/^{86}Sr$). Geochemical and isotopic indicators in shallow groundwater are interpreted in the framework of existing data on geology and soil gasses.

The aim of this study is to investigate direct or indirect near-surface indicators of the presence of deep CO_2 in shallow groundwater, and, in particular, to detect geochemical anomalies that could be linked to CO_2 leakage. The target of the study is shallow groundwater above the natural CO_2 accumulation, based on the postulate that any CO_2 leakage would induce modifications of the geochemical signature of the impacted water. Deciphering the geochemical signature of shallow groundwater should help to better understand water and gas migration accompanied by water-rock interaction. Two main objectives are highlighted: (i) to identify the geochemical pathways leading to the observed water chemistry through environmental isotopes (C, O, H, Sr) in order to (ii) detect any natural CO_2 leakage from the deep CO_2 reservoir or demonstrate that there is no leakage.

Above a CO_2 geological storage site dominated by carbonate rocks, the geochemical signature of shallow groundwater (in our case in molassic and alluvial aquifers) can be supposed to reflect the superposition of biogenic, or in case of leaks, geogenic carbon dioxide, and its interaction with aquifer materials.[25] We thus performed geochemical modeling which principally focuses on the carbonate system. Our models take into account two main sets of conditions in the evolution of groundwater in carbonate system: (i) the reaction of carbonate with pure water in equilibrium with a gas phase with a fixed CO_2 partial pressure (pCO_2) and (ii) the reaction of carbonate with pure water that was initially in equilibrium with a carbon dioxide reservoir, and was then isolated from it before carbonate dissolution. These two models are respectively referred to as open and closed systems.[26]

Typically we may consider as open system processes (i) the carbonate dissolution in soil and shallow groundwater in contact with biogenic soil CO_2 but also (ii) the water-gas-carbonate interactions during migration of supercritical or free CO_2. Once infiltrating water becomes isolated from soil CO_2, in particular in confined aquifers, closed system conditions prevail. All degrees of hybrid systems initially open and then closed to gaseous CO_2 can be encountered. Here, we consider different ranges of values for the key parameters, CO_2 partial pressure, isotopic composition of gas and mineral phase, in adequacy with observations at the study site.

Field study

Natural CO_2 accumulation of Montmiral

In the peri-Alpine province of south-west France, a variety of geological environments induce the generation, migration, accumulation, or leakage of CO_2 of magmatic origin, as a consequence of the regional geological history.[15] These CO_2 occurrences are known through springs, mofettes, or boreholes from the Massif Central to the Alps. They are located along major faults in the Massif Central which forms the outcropping basement or are related to the margins or to deep extensional structures of the basin. In this carbogaseous province, the presence of gas in the upper sedimentary reservoirs is due to migration from depth through major fault systems.[27]

Geology

The Montmiral CO_2-rich reservoir is located in the Rhône Valley between the crystalline basement of the Massif Central and the Vercors (Fig. 1) in a Tertiary basin. Gas accumulation occurs between 2400 and 2480 m depth in Hettangien and Rhaetian limestones and Triassic sandstones. Between 2337 m and 1840 m

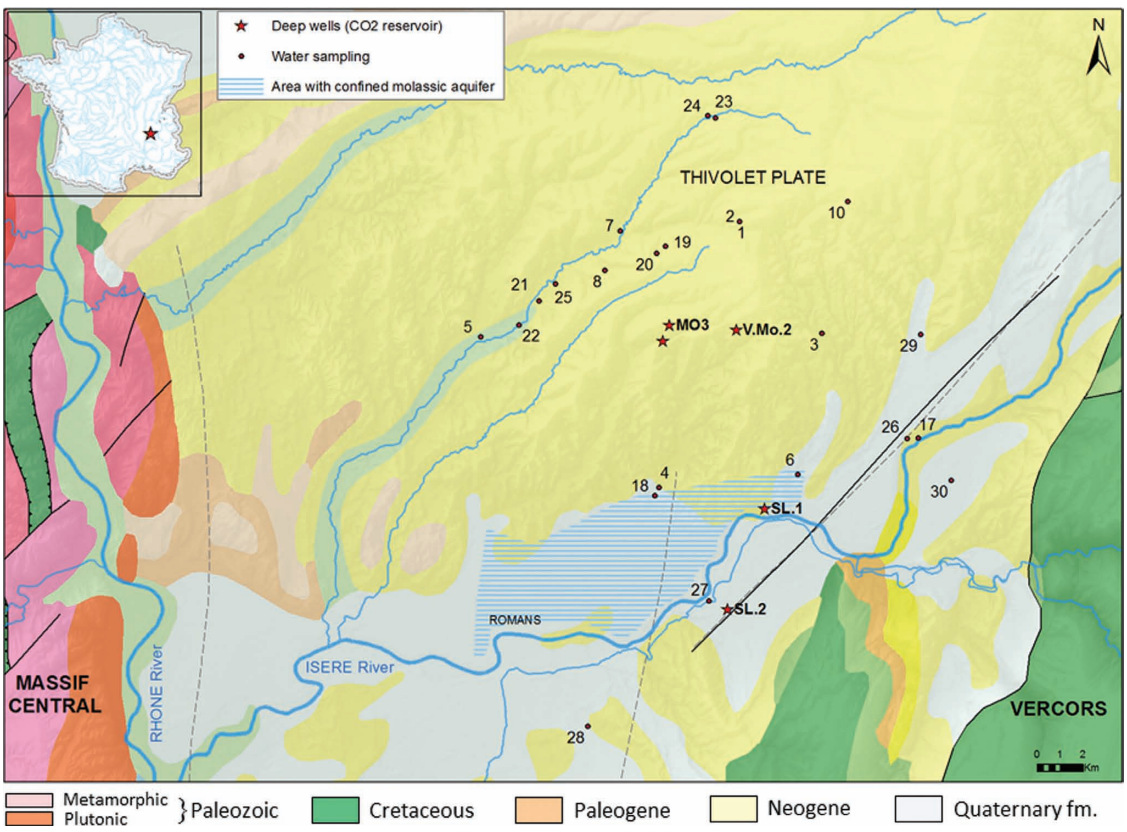

Figure 1. Geological map of the Montmiral area. The tertiary basin (yellow) is located between the basement of the Massif Central (red) and the cretaceous relief of Vercors (green). Localization of the sampling points (1 to 30) and deep wells (V.Mo.2 is the production well). Molassic aquifer is confined within the Eastern part of Romans (modified from de la Vaissière[28]). All the groundwater flows converge towards the Isere Valley.

depth, the reservoir is sealed by caprocks of Domerian to Callovian (clay and marl). This reservoir was exploited as an industrial source of CO_2 for almost two decades.

In the Montmiral area, the Alpine folding led to the formation of anticlines covered by Neogene and Quaternary formations (500 to 600 m thick). These formations fill the succession of molassic foreland basins formed during the Miocene. More precisely, the investigated area is situated within marly fluvio-lacustrine deposits of the upper regressive unit of the Tortonian age. The sediments consist mainly of shallow marine sand and clays.

Hydrogeology

Regionally, fresh groundwater is located in the Miocene and Quaternary formations. At shallow depth, fresh groundwater belongs to the alluvial plain of the Isere River and at greater depth is located in the Miocene molassic layers. This molassic aquifer is the main regional groundwater reservoir. It is a multilayered formation composed of sands, sandstones, clays and marls (carbonate cemented) with a maximum thickness of 600 m. The basal molassic layer is mainly composed of clays and marls.

General groundwater flow is from the East to the West of the plain and follows the topography.[28] Recharge areas are the Chambaran and the Thivolet plateau. All the flow lines converge toward the Isere Valley which is the discharge area.

Radiocarbon dating showed an increase of the residence time from East to West related to an increase of the magnesium content.[28] The groundwater ages increase from modern to 4000 years along a flow path of 10 km and the ground water velocity is around 10 to 20 m/yr. De la Vaissière[28] highlighted a stratification of water flow, with young superficial waters overlying deep old waters. However, in the Isere Valley, old groundwater discharges from the underlying molassic aquifer. Moreover, the author showed that in the Romans area, the molassic aquifer was confined due to the presence of argillaceous layers (Fig. 1).

Previous studies on deep CO_2 leaks

Noble gases, radon, CH_4, gaseous CO_2 and its $\delta^{13}C$ were analyzed in soils by Gal *et al.*[29] whereas the study by Lafortune *et al.*[30] focused on dissolved noble gases and $\delta^{13}C$ of dissolved inorganic carbon in groundwater. Even if CO_2 fluxes, CO_2 soil concentrations, and soil radon activities are, in some places, significant and seem to exceed the natural background range of CO_2 fluxes produced by biological activity, there is no isotopic evidence of non-biogenic CO_2 in soils.[29]

Lafortune *et al.*[30] postulated CO_2 leakage through a deep well, based on the evolution of the ratio He/Ne in the deeper aquifer but, again, the associated evolution of the carbon signature gave no clear evidence of such a leak. In fact, they highlighted that in the deeper water samples, the noble gas signature of the deep reservoir is recognized. The observation of a relationship between the $^4He/Ne$ ratios and the distance to the wells that reach the CO_2 reservoir is interpreted as the consequence of the deep reservoir gas leaking into the shallow aquifers via a poorly sealed well (abandoned since 1956). This suggests that geochemical investigations of local aquifers are as important as those conducted on soil gas to understand migration pathways of gases.

Materials and methods

Twenty-nine water points were sampled among springs, wells, and pits (Table 1) representative of superficial and deep groundwater from the molassic aquifer. Figure 1 illustrates the localization of the water sampling point and the regional hydrogeology.

Concentrations were determined in water samples by inductively coupled plasma-atomic emission spectrometry (ICP-AES) for Ca^{2+}, Na^+, K^+ and Mg^{2+}, and by ion chromatography for Cl, NO_3^- and SO_4^{2-}. The accuracy of both techniques was around 5–10% depending upon the concentration.

Trace element concentrations were measured by inductively coupled plasma mass spectrometry (ICP-MS) (uncertainty 5%). Alkalinity was determined by HCl titration and Gran's method.

The isotopic compositions of hydrogen, oxygen and carbon are expressed in the usual delta notation as a per mil (‰) deviation of the heavy-to-light isotope abundance ratio ($^2H/^1H$, $^{18}O/^{16}O$, and $^{13}C/^{12}C$) in the sample from a standard, oxygen and hydrogen isotopes as $\delta^{18}O$ and δ^2H with respect to the V-SMOW standard, carbon isotopes as $\delta^{13}C$ with respect to the PDB standard.

Oxygen and hydrogen isotopes were determined on a Finnigan MAT 252 mass spectrometer following the gas-water equilibration technique of Epstein and Mayeda[31] and Oshumi and Fujini.[32] All samples were

Table 1. Water sampling point, chemical properties and calculated pCO_2 using PHREEQC.

Sampling Point	N #	Type	Aquifer	depth m	Date	pH	T °C	cond µs/cm	Eh (NHE) mV	pCO2 atm
Pupard Nord	1	*spring*		0	May-02	5.8	11	93	416	$10^{-1.28}$
Pupard Sud	2	*spring*		0	May-02	6.0	11	190	456	$10^{-1.55}$
Pont du Bateau	3	*well*	*molassic*	120	May-02	7.3	13	521	408	$10^{-1.87}$
Les Aygalades	4	*well*	*molassic*	247	May-02	7.3	18	544	378	$10^{-1.74}$
Cabaret neuf 3	5	*well*	*molassic*	155	May-02	7.5	16	395	368	$10^{-2.13}$
Les Sablières	6	*well*	*molassic*	100	May-02	7.7	15	439	245	$10^{-2.31}$
Les 4 Routes	7	*pit*	*molassic*	4	May-02	7.4	14	510	359	$10^{-2.00}$
Chenevrier	8	*spring*		0	May-02	7.2	12	448	396	$10^{-1.89}$
Queue du Furand n°1	10	*spring*		0	Aug-02	7.1	12	383	371	$10^{-1.82}$
Queue du Furand n°2	11	*spring*		0	Aug-02	7.1	14	387	414	$10^{-1.83}$
Queue du Furand n°3	12	*spring*		0	Aug-02	6.7	13	313	374	$10^{-1.52}$
Queue du Furand n°5	13	*spring*		0	Aug-02	7.1	13	454	433	$10^{-1.77}$
Queue du Furand n°6	14	*spring*		0	Aug-02	6.9	14	563	429	$10^{-1.43}$
Queue du Furand n°8	15	*spring*		0	Aug-02	7.1	14	561	425	$10^{-1.66}$
Queue du Furand n°9	16	*spring*		0	Aug-02	7.1	13	584	440	$10^{-1.65}$
Les Fontaines Pétrifiantes	17	*spring*		0	Aug-02	8.0	14	515	367	$10^{-2.69}$
Les Guilhomonts	18	*well*	*alluvial*	34	Aug-02	7.5	20	525	389	$10^{-2.03}$
Les Fagoutières	19	*spring*			Aug-02	7.3	19	364	428	$10^{-2.03}$
Les Magnards	20	*spring*		0	Aug-02	7.3	18	388	428	$10^{-2.04}$
Les Rogières	21	*well*	*molassic*	102	Aug-02	7.0	14	675	340	$10^{-1.65}$
Clamot	22	*well*	*molassic*	87	Aug-02	7.3	14	475	390	$10^{-2.04}$
La Dérine	23	*drain*			Aug-02	6.7	13	183	470	$10^{-1.83}$
La Verte	24	*drain*		0	Aug-02	7.4	13	387	408	$10^{-2.11}$
Les Cabinières	25	*well*	*molassic*	120	Aug-02	7.5	14	376	408	$10^{-2.14}$
Cotton et Grillot	26	*spring*		0	Aug-02	7.1	13	626	420	$10^{-1.72}$
L'Écancière	27	*spring*		0	Aug-02	7.1	13	757	443	$10^{-1.69}$
Le Pinet / le Goubet	28	*well*	*molassic*	210	Aug-02	7.2	15	554	419	$10^{-1.82}$
La Scie	29	*well*	*alluvial*	25	Aug-02	7.1	18	616	445	$10^{-1.67}$
Chirouzes	30	*well*	*alluvial*	24	Apr-00	7.3		699		$10^{-1.77}$

analysed in duplicates. Analytical uncertainty, based on replicate analyses of international and laboratory standards, are ±0.8 ‰ for δ^2H and ±0.1 ‰ for $\delta^{18}O$.

Chemical purification of strontium for isotopic analysis was performed using an ion-exchange column (Sr-Spec) according to a method adapted from Pin and Bassin,[33] with total blank <1 ng for the entire chemical procedure. After chemical separation, around 150 ng of Sr was loaded onto a tungsten filament with a tantalum activator and analysed with a Finnigan MAT 262 multi-collector thermal ionisation mass spectrometer (TIMS). The measured $^{87}Sr/^{86}Sr$ ratios were normalised to an $^{88}Sr/^{86}Sr$ of 0.1194 and then adjusted to the NBS987 standard value of 0.710240. An average internal precision of $\pm 8.106 \times 10^{-6}$ ($2\sigma_m$) was obtained during this study and the reproducibility of the $^{87}Sr/^{86}Sr$ ratio measurements was tested through repeated analyses of the NBS 987 standard for which we obtained a mean value of 0.710227 ± 13 (2σ; n = 18) during the period of analysis.

The C isotope composition of CO_2 gas and dissolved inorganic carbon (DIC) was determined by standard isotope ratio mass spectrometry. Carbon isotopes are

reported as $\delta^{13}C$ in ‰ relative to the PDB standard, with an analytical uncertainty of <0.1‰.

Groundwater composition

Chemical composition of water

Physico-chemical parameters of the sampled waters are provided in Table 1. Spring waters show a wide range of conductivities (100 to 800 µS/cm) and the pH values range from 5.8 to 8. The parameters of the molassic aquifer (well#3 to 7, 18, 21-22, 25, 28) and from the alluvial aquifer (well#18, 29-30) are relatively homogeneous with conductivity ranging from 400 to 700 µS/cm. Regarding the redox potential, all the waters are oxic (340–470 mV) except for the well#6 containing semi-oxic waters (245 mV, NHE).

Groundwater is of the Ca-HCO_3- type or Ca-Mg-HCO_3- type except for the Spring #2 whose anions are dominated by the presence of nitrates.

The anthropogenic impact on superficial waters is important in the Isère plain where agriculture is the main economic activity. Alluvial waters (wells#29-30), numerous springs (#2,26,27) and some molassic groundwater (wells#3,21,22,25) can have high concentrations in NO_3^- (up to 0.73 mmol.l^{-1}). The wells# 4, 5 and 18 are not influenced by human activities with NO_3^- concentrations below 0.05 mmol.l^{-1} (Table 2).

High sulfate concentrations may naturally originate from evaporites but another possible source is gypsum used for soil improvement or in fertilizers. In fact, relatively elevated values are observed in superficial wells #29-30, in the well #21 (molassic well) and springs #17,26,27. In the Isère valley, intense pressure from agriculture is also reflected in superficial groundwater by the presence of pesticides.[28]

The system is clearly dominated by interaction of carbonic acid with the carbonate rocks of the aquifer material (Fig. 2). For most springs and groundwater, the equivalent ratio of Ca, corrected for gypsum dissolution assuming that this is the sole source of sulfate, and HCO_3^- is close to 1 indicating stoichiometric calcite dissolution as principal mechanism. The falloff from the 1:1 line in Fig. 2 is greatest for the most nitrate-polluted groundwater (#21, 27, 30). A distinct group of waters (#4,5,6,18) plots close to the 1:2 line of stoichiometric dolomite dissolution. Those are indeed the waters with Ca-Mg-HCO_3^- type and molar Mg/Ca ratios close to 1.

The same group of waters (#4,5,6,18) is enriched in Na compared to Cl whereas the springs (above 0.1 mmol Cl.l^{-1}) and wells fall below the theoretical marine ratio (Fig. 3). As the local rocks are evaporite-free, the only Cl sources are rainfall and anthropogenic inputs. Considering an average evaporative enrichment factor (1.5), concentrations up to 0.09 mmol.l^{-1} can be considered as originating from rainfall (Cl in rainwater in Avignon:[34] 0.037 mmol.l^{-1}). The anthropogenic origin of higher Cl^- concentrations is confirmed by the correlation with NO_3^-.

Regarding the four wells (# 4, 5, 6, 18), Mg-enrichment, which is accompanied by a Na-excess with respect to Cl, is an indicator for water-rock interactions. The Na-enrichment points to base exchange on clay minerals inducing depletion in bivalent cations or to dissolution of Na-bearing silicates, for example, albite. The molar Mg/Ca ratios of this group are higher by a factor of 20 than the average of the other points and exceed, in the case of 4, 6, and 8, a value of 1. Such high values can be due to dolomite dissolution,[28] dolomite being present in the aquifer matrix of molasse sediments.[35] Mg/Ca ratios close to equity have also been observed for the deep parts of the Chalk aquifer[36,37] and were explained by incongruent dissolution of Mg-rich calcites of the chalk matrix. Mg-enrichment with respect to Ca masks any potential effect of cation exchange on Ca as Na+K are minor (<10%) compared to Ca+Mg. These interactions are mainly observed in the deeper wells potentially draining older waters thus increasing the time of interaction with the aquifer matrix. The well #18 also shows this enrichment while it is identified as a superficial well (34 m deep, screening in the alluvial formations). In fact, in this area, de la Vaissiere[28] showed that the molassic aquifer is confined and deeper waters could rise and mix with shallow groundwater so that the composition could be close to the composition of deep waters observed in the well #4 (247 m deep).

Isotopic composition of water and dissolved CO_2

Regarding the stable isotope data of water, δ^2H and $\delta^{18}O$ isotope composition of groundwater is –62‰ to –56 ‰ and –9.4 ‰ to –8.2 ‰ respectively (Table 2). In Fig. 4, two local meteoric lines (LMWL, respectively Nimes and Avignon, France) from Blavoux and Berthier[38] and Celle *et al.*[39] are plotted. Water sampling points are located along the local meteoric lines and the global meteoric water line.

Table 2. Chemical and isotopic analysis of groundwater.

#	Date	HCO3 (mg/l)	Ca (mg/l)	Mg (mg/l)	Na (mg/l)	K (mg/l)	Cl (mg/l)	NO3 (mg/l)	SO4 (mg/l)	Fe (mg/l)	Mn (µg/l)	Si (mg/l)	$\delta^{18}O$ ‰ vs. V-SMOW	$\delta^{2}H$ ‰ vs. V-SMOW	$\delta^{13}C$ ‰ vs. PDB	87Sr/86Sr
1	May-02	37	16.1	0.6	1.4	0.6	3.7	7.5	1.8	<0,02	6	8.6	–9.2	–61.4	–16.2	0.709787
2	May-02	35	31.4	1.6	2	2	10.3	36.3	3.9	<0,02	5	8	–8.9	–59.8	–15.6	0.710052
3	May-02	299	102	6.6	3.8	1.1	8.4	20.9	12.3	<0,02	<5	11.7	–8.7	–59.4	–12.1	0.708424
3b	Nov-00	291	105	<0,01	3.6	0.9	8.3	20.4	11.4		<10	13.1				
4	May-02	371	55.4	39	10.6	1.2	2	1.9	6.2	<0,02	<5	22.9	–8.8	–59.7	–10.5	0.708821
4b	Nov-96	359	47.7	35.9	10.8	–	1.3	3	2							
5	May-02	269	57.1	20.1	6.2	1.1	2.1	1	3.7	<0,02	6	17.8	–8.8	–58.2	–8.6	0.708683
6	May-02	255	33.3	33.5	12	2	3.7	13.9	6.6	0.03	5	15.6	–8.7	–59.5	–8.6	0.709475
7	May-02	313	110	3.5	3.7	1.4	8.4	8.6	11	<0,02	<5	7.4	–8.6	–57.9	–13.6	0.70847
8	May-02	237	94.9	1.5	2.7	1.3	8	27	7.4	<0,02	<5	11.3	–8.7	–57.3	–14.8	0.708252
10	Aug-02	224	76	1.1	1.8	0.5	2.8	3.3	4	<0,02	<5	10.4	–9.3	–61.1	–13.5	0.708021
11	Aug-02	218	75.9	1	1.8	0.6	4.3	2.4	4.4	<0,02	<5	11.5	–9.3	–61.7	–13.6	0.70803
12	Aug-02	181	61	0.8	1.4	0.5	2.3	0.5	3.6	<0,02	<5	10.2	–9.2	–61	–14.9	0.708049
13	Aug-02	249	92.8	1.1	1.5	0.5	2.8	2.9	4.2	<0,02	<5	10.5	–9.2	–60.9	–14.3	0.708198
14	Aug-02	343	117	1.6	1.8	1.1	3.1	3.3	4.7	<0,02	<5	11.2	–9.3	–61.8	–14.2	0.708155
15	Aug-02	294	115	1.3	1.5	0.7	7.2	16.1	7.7	<0,02	<5	9.8	–9	–59.5	–14.4	0.708018
16	Aug-02	323	118	2.3	1.9	1.2	6.7	13.4	9.8	<0,02	<5	9.7	–9	–60.7	–14.5	0.708197
17	Aug-02	230	95.3	6	7.9	1.7	16.6	25.4	19.1	<0,02	<5	14.4	–8.7	–58.7	–10.7	0.708433
18	Aug-02	296	46.3	33.9	15.1	1.4	1.7	1.5	7.1	<0,02	<5	27.9	–9.2	–60.9	–10	0.708864
19	Aug-02	186	71.9	1.5	2.2	0.7	5.6	3.7	3	<0,02	<5	13.8	–9.2	–60.8	–14.7	0.708466
20	Aug-02	195	77.1	1.3	3.1	0.9	6.1	9.6	3	<0,02	<5	13.9	–9.1	–60.1	–14.6	0.70838
21	Aug-02	297	135	2.7	4.1	1	16.7	33.2	20.5	0.02	6	11.7	–8.4	–56.1	–13.5	0.708551
22	Aug-02	220	92.6	2.8	2.7	1.2	7.8	24.4	11.5	<0,02	<5	12.5	–8.8	–58.3	–12.5	0.708431
23	Aug-02	94	34.3	0.8	2	0.8	1.9		0.5	<0,02	<5	13.8	–9.3	–60.9	–15.1	0.708435
24	Aug-02	231	80.1	1	1.4	0.9	2.9	0.8	2.3	<0,02	<5	12.5	–9.1	–59.8	–13.9	0.708077
25	Aug-02	281	128	2.3	3.7	1.1	16.6	33.3	18.4	<0,02	19	12.3	–8.7	–57.1	–12.3	0.708433
26	Aug-02	297	119	4.7	6.4	1.7	13.6	27.7	14.8	<0,02	<5	15.4	–8.6	–58.2	–12.3	0.70835
26b	Mar-00	319	119	<0,01	7.24	1.38	19	24	14	<0,05	<10	12.6				
27	Aug-02	339	144	7.7	4.6	1.7	11.3	45.2	20	<0,02	<5	13.5	–8.2	–55.9	–12.4	0.708181
28	Aug-02	286	99.3	10.8	4	1.1	6.6	18.4	4.9	<0,02	<5	17.5	–8.3	–55.6	–11.6	0.708173
29	Aug-02	300	119	4.8	4.3	2.9	12	15	16.4	<0,02	<5	11.1	–8.7	–58.2	–12.9	0.708217
29b	Mar-01	339	126	4.8	3.9	1.3	13.7	17.1	16.4	0.05	<10	9.8				
30	Apr-00	383	155	<,01	6.45	1.44	19.1	41.6	48	<,05	<10	10.1				

Some of the spring waters show a small deviation from the local meteoric lines (Fig. 4(a)). Two types of oxygen-18 'exchange' reactions may occur during the carbo-gaseous groundwater flow, one with the reservoir matrix and the other with gaseous CO_2 which may impose its signature if it is present in abundance. These reactions would not change the deuterium content of the water, hydrogen being absent from the CO_2 gas and scarce in the rocks (Fig. 4(b)). A position left of the local meteoric water line is frequently observed in for thermo-mineral waters in the Massif Central and supposed to reflect the isotopic exchange of the water's oxygen with that of the CO_2.[40–42] Based on an isotopic mixing model, considering measurement uncertainty, it is possible to determine the fraction

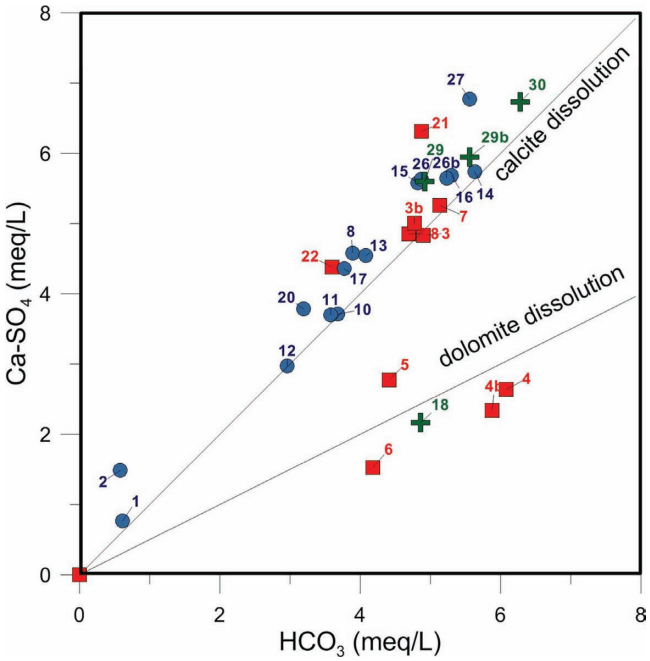

Figure 2. Ca corrected for SO_4^{2-} vs. and HCO_3^- (in meq.l^{-1}). Stoechiometric calcite and dolomite dissolutions are also reported.

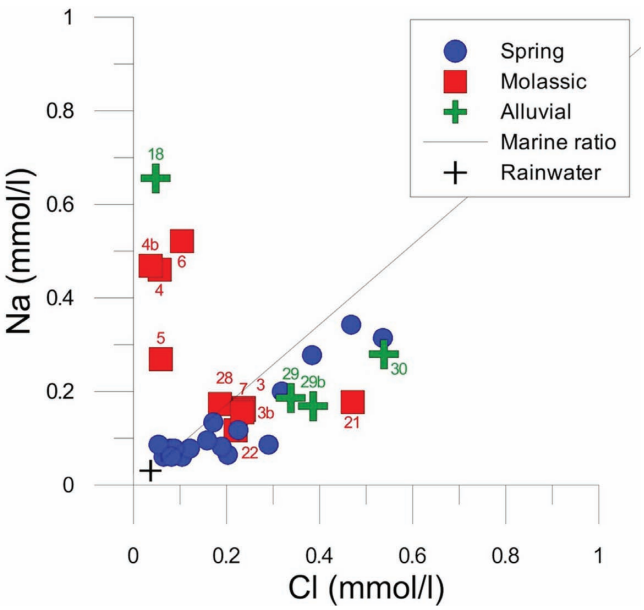

Figure 3. Na concentration versus Cl concentration.

of oxygen from CO_2 contributing to the oxygen of the water molecule.[43,44] If we consider that the oxygen sources in the medium are the oxygen of the initial water H_2O and of the CO_2, the resulting equation is:

$$\delta^{18}O^{f}_{H_2O} = \delta^{18}O^{i}_{H_2O} \times \left(1 - X_{O\_CO_2}\right) + \left(\delta^{18}O^{i}_{CO_2} - \varepsilon_{CO_{2(g)}-H_2O}\right) \times X_{O\_CO_2} \quad (1)$$

with $X_{O\_CO_2}$ being the mole fraction of the CO_2 oxygen relative to the total oxygen, and the exponents f and i indicating the final and initial isotopic values, respectively, $\varepsilon_{CO_{2(g)}-H_2O} (= \varepsilon^{18}O^{f}_{CO_{2(g)}} - \delta^{18}O^{f}_{H_2O} = +40.1‰$ at 20 °C)[45] is the enrichment factor.

The isotopic composition of the deep CO_2 from Montmiral reservoir is $\delta^{18}O^{i}_{CO_2} = +25$ ‰ vs. SMOW.[24] The results show that the greater the amount of CO_2 in the system, the more the final water with $\delta^{18}O^{f}_{H_2O}$ is depleted in ^{18}O ($\delta^{18}O^{f}_{CO_2}$ increases and becomes enriched in ^{18}O in compensation). The contributing mole fraction of CO_2 oxygen to the total oxygen necessary to obtain, the highest observed negative shift of $\delta^{18}O$ from the LMWL in our system of $\left|\Delta\delta^{18}O_{H_2O}\right| = 0.3 \pm 0.2$‰ is around 2–5%. We can conclude that the gas-water ratio was not sufficiently high to induce a significant isotopic exchange.

$\delta^{13}C$ values of DIC vary between –16.2 ‰ to –8.5 ‰ PDB (Table 2), a moderate range of variation compared to regional investigation of Blavoux and Dazy [27] who recorded values as high as –4.1‰. From a biogenic source we would expect CO_2 typically at –20 to –25‰, whereas the recorded $\delta^{13}C$ must be derived, at least partially, from a ^{13}C-enriched source of carbon. With a $\delta^{13}C$ of deep CO_2 at –2.7 ‰,[24] leaks from the reservoir could represent this ^{13}C-enriched end-member. Other candidates are marine carbonates contained in the molassic formation. De la Vaissière[28] reported isotopic signatures of carbon in a variety of rocks from the investigated sedimentary basin. In the molassic formation, values range from –2.35 ‰ to –5.13 ‰ vs. PDB, in Oligocene carbonates (Urgonian) from 0.58‰ to –1.24 ‰ vs. PDB.

Actually, the waters with the most enriched in ^{13}C (samples # 5 and 6) plot to the right of the local meteoric water line in the ($\delta^{18}O$, $\delta^{2}H$) diagram, which excludes any significant exchange between water and CO_2 of deep origin.

Trace element geochemistry

Analyses of groundwater for trace elements were conducted with the double objective to identify

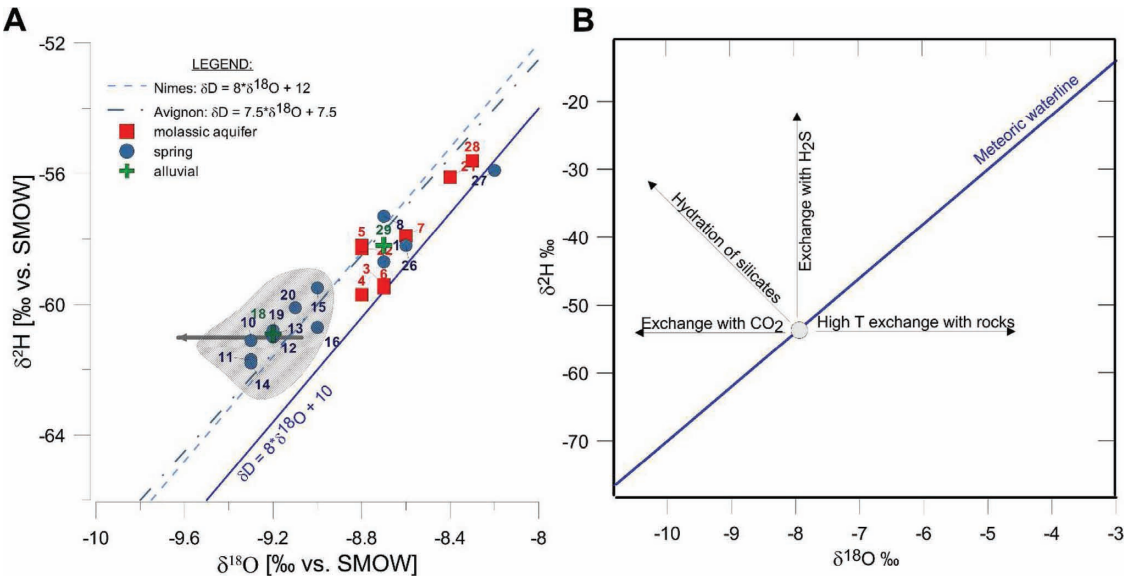

Figure 4. (a) Stable isotopes of the water molecule $\delta^{18}O$ vs. $\delta^{2}H$ with global and local meteoric water lines.[38,39] (b) Principal processes that can deviate water from the meteoric water line.

appropriate tracers of CO_2 leaks and to assess the impact of CO_2 leaks on groundwater quality. Average concentrations of trace elements have been calculated for all elements as well as the range of variation expressed by the 10th and 90th percentile (Fig. 5). Variations exceed an order of magnitude for only few trace elements (Cu, Pb, Cr, Zn) which therefore are not more significant than those of major elements like Na, Ca, Cl, or NO_3. No anomaly regarding the natural background or particularly elevated concentrations of any trace element or group of elements can be noticed. The comparison between the less and most ^{13}C enriched samples from the molassic aquifer (#7,21 and 4 to 6) does not show any significant trace

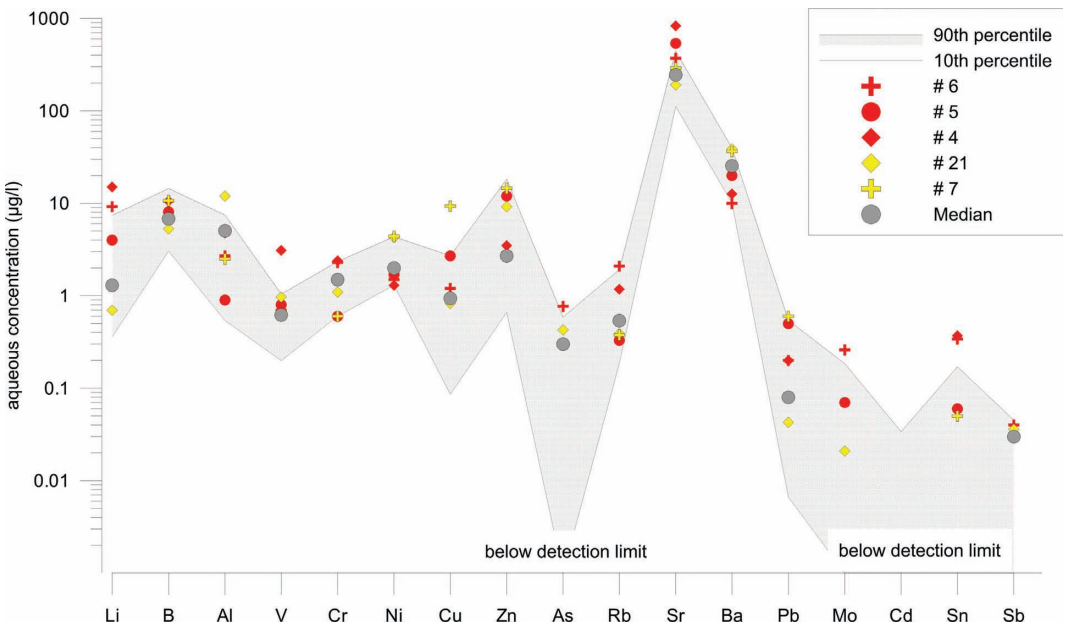

Figure 5. Trace element patterns of groundwater (in µg/l).

element increase associated with the enrichment in ^{13}C. One can only notice that the ^{13}C enriched samples are also enriched in Sr that is released by carbonate dissolution. On the contrary, the most ^{13}C-enriched samples 5–6, present for some elements concentrations below those of the most ^{13}C-depleted sample (Ni, Cd, Ba). Previous studies predict an important impact of CO_2 leaks on trace elements (Pb, As) concentrations which may exceed drinking water quality limits.[46,47] As a consequence of the CO_2 injection experiment conducted at Frio, Kharaka *et al.*[48] observed dissolution of iron oxy-hydroxides leading to an increase of Fe, Mn, Zn, and Pb concentration. For the groundwaters sampled above the CO_2 reservoir of Montmiral, such anomalies cannot be observed: the Fe concentration of the most ^{13}C enriched sample is lower than average concentrations in the area and concentrations of Mn, Pb, As, and Zn match with average background concentrations.

Geochemical speciation and calculated pCO_2

Using Phreeqc,[49] aqueous speciations were calculated for all measured groundwater chemistries with the database Thermoddem.[50] All calculations consider water temperature, pH and the redox potential measured *in situ* during the groundwater sampling campaign.

Partial pressure of CO_2 (pCO_2) was calculated for all samples based on measured pH and alkalinity (Table 1). pCO_2 values range between $10^{-2.59}$ and $10^{-1.28}$ atm by a factor 6 to 160 higher than atmospheric $pCO_2 = 10^{-3.5}$ atm. pCO_2 is well correlated with DIC except for springs #1 and 2 that have higher pCO_2 relative to DIC concentration. No distinction is observed between boreholes and springs, or alluvial and molassic groundwater. In fact, deepest waters (#5,6 and #18) are not the most alkaline and pCO_2 is relatively low for these wells (10^{-2} to $10^{-2.3}$), while spring #1 and 2 presents higher pCO_2 ($10^{-1.28}$ and $10^{-1.55}$ atm, respectively).

The saturation indices (SI) show minerals with which groundwater is potentially in equilibrium (Fig. 6). All waters except for the spring #1 and 2 and the drain #23 are equilibrated with respect to calcite. This equilibrium is rapid to obtain and the calculation of this equilibrium confirms that pH and alkalinity were correctly measured *in situ*. Even the deepest waters (#4,5,6,18), with their low pCO_2 values, are in thermodynamic equilibrium with calcite and dolomite (Fig. 6). Regarding the spring #17, water is oversaturated with respect to calcite and dolomite, which is coherent with the precipitation of travertine observed around the spring. The waters from spring #1 and 2 are undersaturated ($SI_{calcite} < -2$) with respect to carbonate minerals which indicates that waters

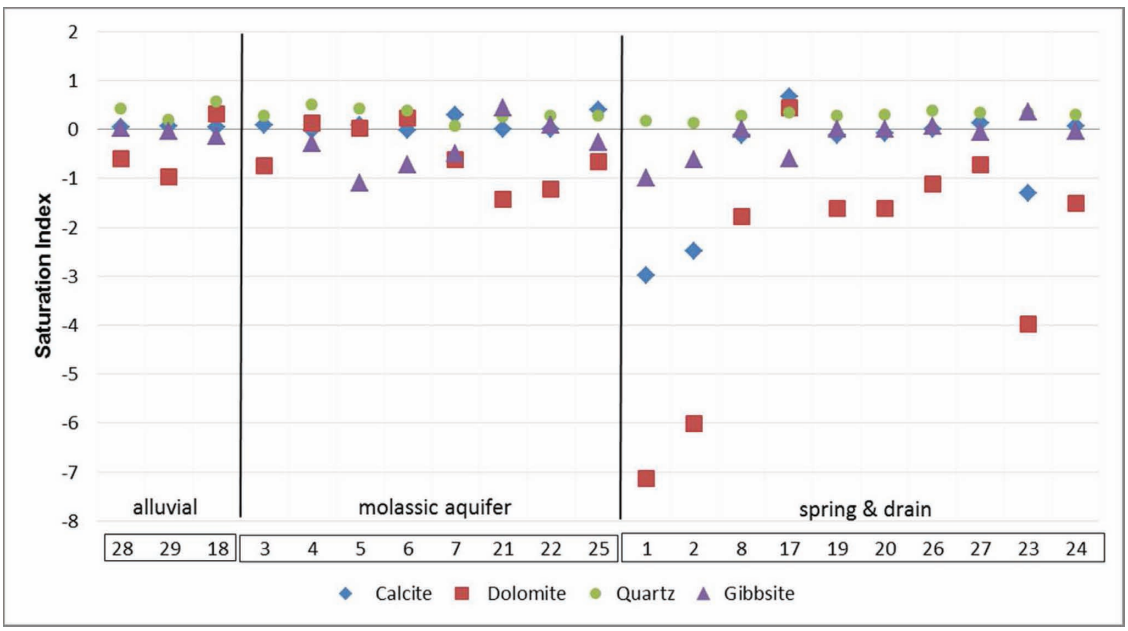

Figure 6. Saturation indices of waters with respect to main minerals.

were probably not or only briefly in contact with calcite.

All the waters are close to equilibrium with respect to quartz and chalcedony. Regarding clays (kaolinite, illite, montmorillonite), waters are clearly over-saturated. These waters are in equilibrium with gibbsite so that aqueous silica is probably controlled by chalcedony and Al by gibbsite.

For #3 and 8, the indices for alumino-silicates are not calculated as the Al-concentration is below the detection limit. For #19 and 20 no data are available for trace elements. Waters containing iron (# 6, 21) are oversaturated (SI ~ 5.5) with respect to goethite. This indicates that iron is present as Fe^{III} (oxidized state) and probably present as colloid (<0.45 μm, filtration rate). Due to their surface properties, Fe and Al-oxy-hydroxydes can adsorb trace elements which can be released in case of pH decrease due to CO_2 intrusion.[2,4,46] However, as shown previously, no anomaly for Al, Fe or other trace elements is observed in the groundwater.

Isotopic approach and evolution of the carbonate system

Chemical and isotopic constraints

As previously highlighted, the chemistry of water is controlled by carbonate dissolution. Changes in water chemistry during carbonate dissolution are accompanied by changes in the $^{13}C/^{12}C$ ratios of the groundwater DIC.

The approach used to model the evolution of chemical and isotopic composition during carbonate rock dissolution takes into account the chemical and isotopic composition of water in equilibrium with a carbon dioxide reservoir with a given partial pressure (pCO_2) and the isotopic signature of gas ($\delta^{13}C_{CO2(g)}$). After this initial equilibration step, the resulting solution reacts with carbonate of a given isotopic composition ($\delta^{13}C_m$) under open or closed compositions.[26,35,51,52]

Open system As described by Deines *et al.*,[26] during the process of carbonate dissolution in an open system the water remains in contact with a sufficiently large and homogeneous reservoir of CO_2 of fixed partial pressure and the isotopic and chemical equilibrium is maintained between DIC and the CO_2 reservoir during dissolution.

The relative proportions of H_2CO_3, HCO_3^- and CO_3^{2-} change as a function of pH. The total DIC represents the sum of these species. The $\delta^{13}C$ of groundwater DIC depends on the $\delta^{13}C$ signature of the dissolved gaseous CO_2 and the fractionation with respect to the different carbonate species in the solution. Since $\delta^{13}C_{CO2(g)}$ is assumed constant, the ^{13}C content of the solution during carbonate dissolution will change only through a shift in speciation of total DIC linked to pH evolution and is independent of the mineral $\delta^{13}C$.[26]

The calculation of $\delta^{13}C_{DIC}$ for the open system is described in Eqn (2):

$$\delta^{13}C_{DIC} = \frac{\left(\left[H_2CO_3^*\right]\delta^{13}C_{H_2CO_3^*} + \left[HCO_3^-\right]\delta^{13}C_{HCO_3^-} + \left[CO_3^{2-}\right]\delta^{13}C_{CO_3^{2-}}\right)}{C_T} \quad (2)$$

where $\delta^{13}C$ for $H_2CO_3^*$ (corresponding to $CO_{2(aq)}$ plus H_2CO_3), HCO_3^-, CO_3^{2-} are computed from the equilibrium constants α_0, α_1, α_2 (Eqns 3 to 5). At 10°C, the equilibrium isotope fractionation factors with respect to gaseous CO_2:[26]

$$\alpha_0 = \frac{(^{13}C/^{12}C)_{H_2CO_3^*}}{(^{13}C/^{12}C)_{CO_{2(g)}}} = 0.999 \quad (3)$$

$$\alpha_1 = \frac{(^{13}C/^{12}C)_{HCO_3^-}}{(^{13}C/^{12}C)_{CO_{2(g)}}} = 1.0092 \quad (4)$$

and

$$\alpha_2 = \frac{(^{13}C/^{12}C)_{CO_3^{2-}}}{(^{13}C/^{12}C)_{CO_{2(g)}}} = 1.0075 \quad (5)$$

Closed system For the closed system model, it is assumed that at a given pH, the water is equilibrated isotopically with a gas reservoir of a specified pCO_2 but is isolated from that reservoir before carbonate dissolution begins. In this case, the ^{13}C content of the solution depends not only on the $^{13}C/^{12}C$ ratio of reservoir CO_2 ($\delta^{13}C_{CO2(g)}$) and on pH, but also on that of the dissolving carbonate rock ($\delta^{13}C_m$).[26] The total $\delta^{13}C_{DIC}$ of solution in contact with calcite is calculated as:

$$\delta^{13}C_{DIC} = C_{T,initial}\delta^{13}C_{DIC,initial} + C_m\delta^{13}C_m \quad (6)$$

where

$$C_m = \delta\left[Ca^{2+}\right] = \frac{1}{2}\delta[Alk] \quad (7)$$

and where $\delta^{13}C_{DIC,initial}$ is calculated using Equation 1 and *Alk* is the carbonate alkalinity.

In sum, the geochemical model includes the following steps: (i) infiltrating water will equilibrate with the gaseous phase according to Henry's Law. DIC will be slightly depleted in ^{13}C with respect to the gaseous phase; (ii) the resulting water will dissolve the carbonate matrix under open and/or closed conditions; (iii) once saturation with respect to carbonate rock is reached, isotopic and chemical evolution can continue by incongruent dissolution.

Initial conditions: characterization of gas and mineral phases

According to the measured physico-chemical data and the speciation calculations with PHREEQC (Table 1), we have considered a pCO_2 range from $10^{-1.2}$ to $10^{-2.2}$ atm and a large pH range from 4.0 to 9.0.

The isotopic parameters taken into account are the $\delta^{13}C$ of the $CO_{2(g)}$ and of the carbonate rock. Different sources of carbon dioxide are considered in this study: oxidized biogenic organic matter, plant root respiration, natural deep CO_2.

For a majority of plant species, organic carbon has average $\delta^{13}C$ values around –25‰ [26] but it can be isotopically heavier in case of cultivation of C4 type plants like corn. We have thus considered a $\delta^{13}C$ range from –25‰ to –19‰ for the biogenic CO_2 in accordance with Gal *et al.*[29] and of –2.7‰ for the geogenic CO_2.[24]

The second isotopic parameter required by the models is the isotopic composition of the local carbonate rocks. Based on the values measured by De la Vaissière,[28] we have assumed in our model isotopic compositions between –4 ‰ and 0 ‰.

Modeling results

Congruent and incongruent dissolution processes

The chemical and isotopic changes occurring during carbonate dissolution were evaluated for a large number of different combinations of initial conditions. Some results are given in Fig. 7.

For an open system model, the diagram of log HCO_3^- vs. pH (Fig. 7(a)) shows a set of straight dotted lines which represent dissolution paths for different pCO_2 conditions from $10^{-1.2}$ to $10^{-2.2}$ atm until calcite saturation is reached. Figure 7(b) shows that the ^{13}C content of the DIC increases during the reaction progress. The final ^{13}C enrichment of solution at calcite saturation depends on the pCO_2 during solution and the isotopic composition of gaseous CO_2. Indeed, the ^{13}C content of the dissolving $CaCO_3$ has no influence on the relationships under open system conditions (Eqn 1). If different $\delta^{13}C_{CO2(g)}$ are assumed, isotopic evolution along the dotted lines will change correspondingly. For instance with an initial $\delta^{13}C_{CO2(g)}$ of –2.7 ‰ vs PDB (reservoir gas) and a pCO_2 of $10^{-2.0}$ atm, the solution would have an initial pH of 4.91, a HCO_3 concentration of $1.2{\cdot}10^{-5}$ mol.l^{-1} and a $\delta^{13}C$ of –3.46 ‰ and would attain a $\delta^{13}C$ = +5.59 ‰ at saturation with a pH of 7.3. With the highest considered biogenic initial $\delta^{13}C_{CO2(g)}$ of –19 ‰ and a pCO_2 of $10^{-2.0}$ atm, the DIC would have initial $\delta^{13}C$ of –19.76 ‰ and would attain $\delta^{13}C$ = –10.49 ‰ at saturation.

In contrast, the closed system model shows non-linear dissolution curves in the logHCO_3-pH diagram (Fig. 7(a)). In the $\delta^{13}C$-pH diagram, we observe that the $\delta^{13}C$ varies with the initial pH values but is independent of the initial pCO_2. Different geochemical pathways are represented for different gas and mineral isotopic compositions. For instance, with an initial $\delta^{13}C_{CO2(g)}$ of –2.7 ‰ vs. PDB and a $\delta^{13}C_m$ = 0 ‰, the solution would have initial pH of 4.86, a HCO3 concentration of $1.4e^{-5}$ mol.l^{-1} and a $\delta^{13}C$ of –3.56 ‰ and would attain $\delta^{13}C$ = –1.78 ‰ at saturation with a pH of 8.4. With an initial $\delta^{13}C_{CO2(g)}$ of –19 ‰ vs. PDB and a $\delta^{13}C_m$ = 0 ‰, the solution would have initial $\delta^{13}C$ of –20.01 ‰ and would attain $\delta^{13}C$ = –11.59 ‰ at saturation. This strong potential contrasts provide a clear criteria of discrimination of deep geogenic from shallow biogenic CO_2.

Measured $\delta^{13}C$ and pH values for waters from spring and wells in the study site are plotted in Figs 7(a) and 7(b), along with some expected relationships for open and closed system conditions. The isotopic compositions of the $\delta^{13}C_{DIC}$ in the groundwaters range from –8.6 to –16.1 ‰ vs. PDB. The highest signature (–8.6 ‰) is localized near the SL1 well (#6) and along the Herbasse valley (#5).

A CO_2 gas phase with an isotopic composition between –22‰ and –19‰ explains the majority of the

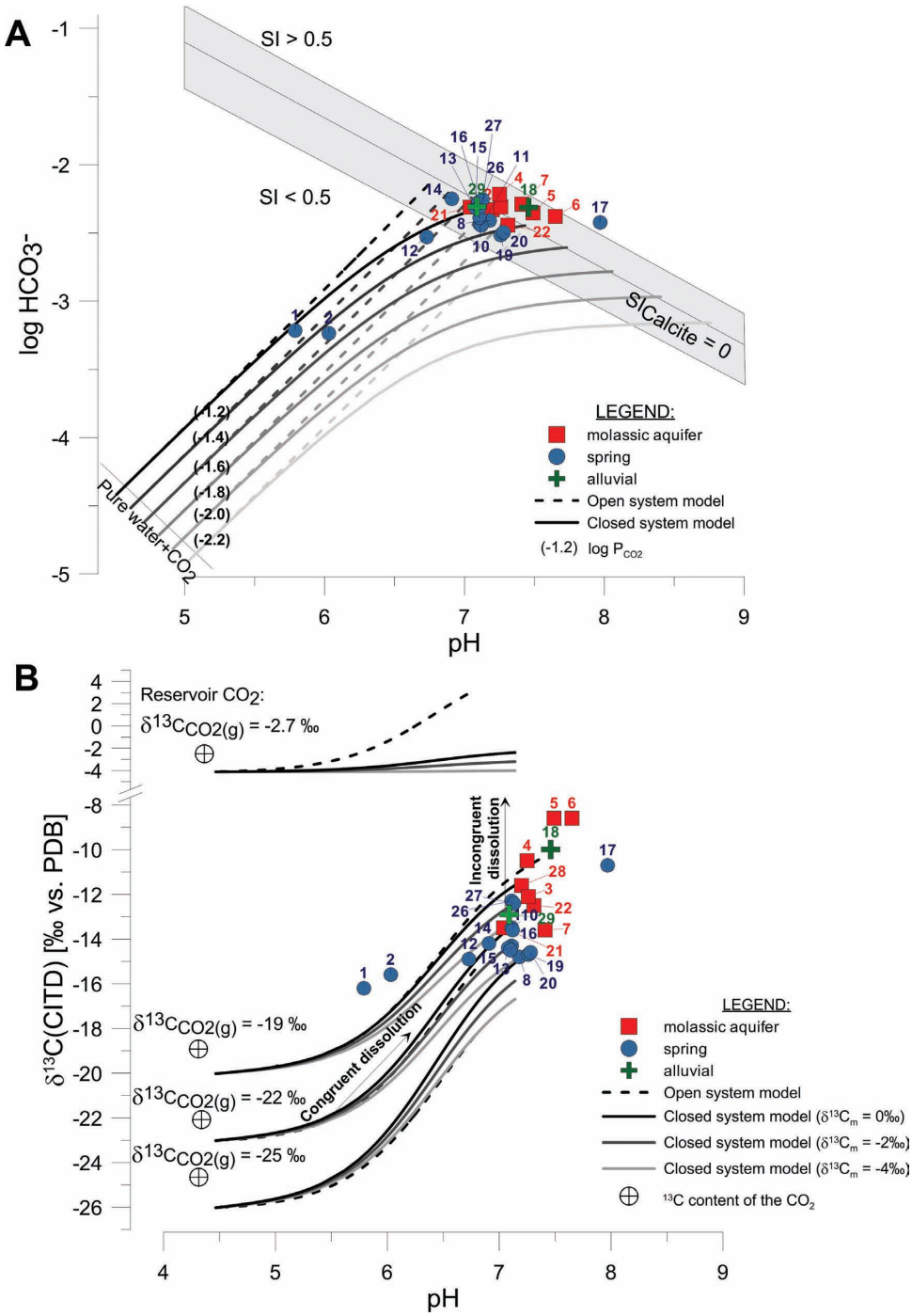

Figure 7. Result of modeling approach in open and closed systems comparison with sampling water points of the study A) log HCO_3^- versus pH and B) $\delta^{13}C_{DIC}$ versus pH.

measured points in the molasses aquifer (Fig. 7(a)). We highlight two potential origins of such an initial value (i) slightly heavier organic matter signature compared to average C3 plants, e.g. with contribution of C4 plants[51] or (ii) a mixed gas phase with a light biogenic end member and a minor fraction of deep geogenic ^{13}C-enriched CO_2 (magmatic origin). Open and closed system solution of carbonate will lead to different $\delta^{13}C$-pH-HCO_3 relationships and hence also different $\delta^{13}C$-Ca relationships. Figure 8 shows the evolution of calcium and $\delta^{13}C_{DIC}$ in our model for different initial conditions. The spring water points and most

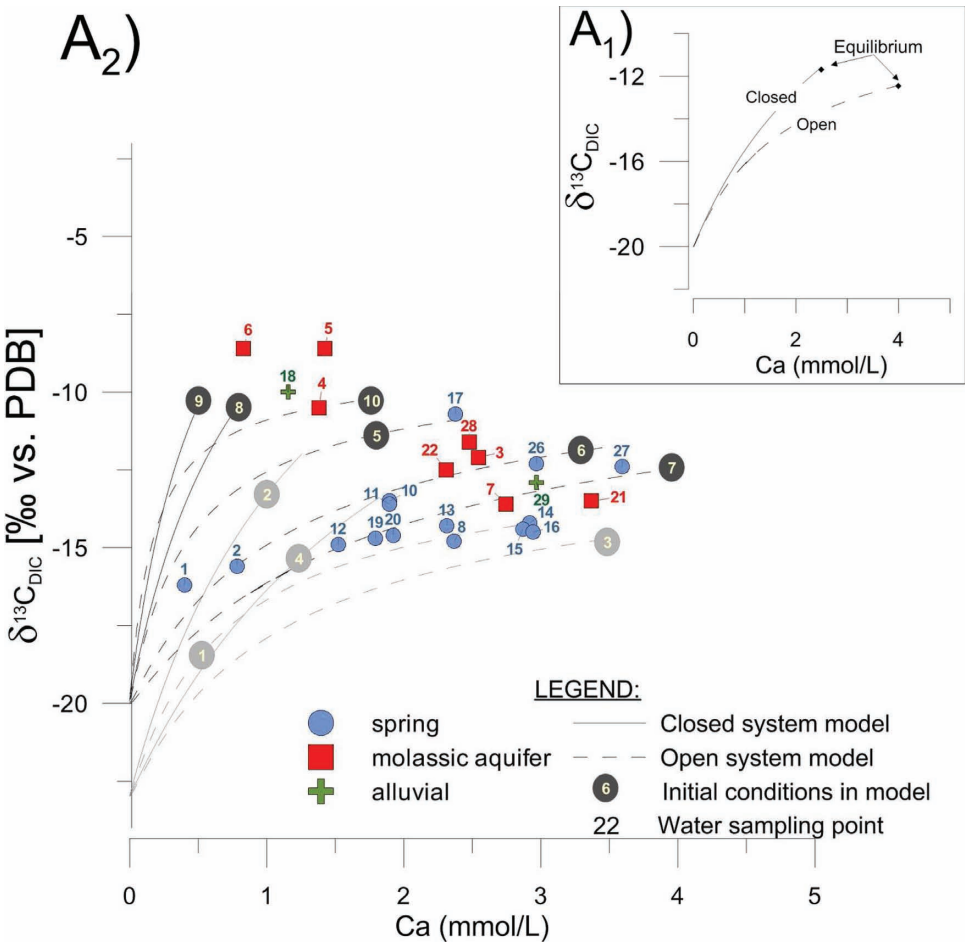

Figure 8. (a1) δ13C of water when calcite dissolves in open or closed conditions with respect to CO_2 gas; example with initial conditions of $\delta^{13}C_{CO2(g)}$ = –19 ‰; log pCO_2 = –1.2; δ^{13}Cm = 0 ‰. (a2) Open and closed system solution paths with initial conditions. ❶ $\delta^{13}C_{CO2(g)}$ = –22 ‰; log pCO_2 = –1.6 ❷ $\delta^{13}C_{CO2(g)}$ = –22 ‰; log pCO_2 = –1.6; δ^{13}Cm = 0 ‰ ❸ $\delta^{13}C_{CO2(g)}$ = –22 ‰; log pCO_2 = –1.4 ❹ $\delta^{13}C_{CO2(g)}$ = –22 ‰; log pCO_2 = –1.4; δ^{13}Cm = –2 ‰ ❺ $\delta^{13}C_{CO2(g)}$ = –19 ‰; log pCO_2 = –1.8 ❻ $\delta^{13}C_{CO2(g)}$ = –19 ‰; log pCO_2 = –1.4 ❼ $\delta^{13}C_{CO2(g)}$ = –19 ‰; log pCO_2 = –1.2 ❽ $\delta^{13}C_{CO2(g)}$ = –19 ‰; log pCO_2 = –1.8; δ^{13}Cm = 0‰ ❾ $\delta^{13}C_{CO2(g)}$ = –19 ‰; log pCO_2 = –2.0; δ^{13}Cm = 0‰ ❿ $\delta^{13}C_{CO2(g)}$ = –19 ‰; log pCO_2 = –2.2.

groundwaters seem to follow a geochemical pathway in open conditions. Yet, the possible isotopic evolution paths during congruent dissolution for different $\delta^{13}C_{CO2(g)}$ values shown, both in Figs 7 and 8, cannot explain all sampling points. For the isotopically enriched samples with high Mg/Ca ratio (4, 5, 6, and 18) another geochemical process must be taken into account.

Dolomite and dolomitization

Figure 8 highlights the importance of incongruent dissolution which may lead to enriched δ^{13}C values approaching –8‰. Leaking deep CO_2 could explain such high values, but we would expect, in this case, enhanced congruent carbonate dissolution with cation ratios in the liquid phase reflecting those of solid carbonates. Though, Fig. 9 shows a clear association of high Mg/Ca ratios with enriched δ^{13}C values. It was shown by Edmunds *et al.*[36] that the bivalent cation ratios Mg/Ca and Sr/Ca are directly related to groundwater residence time. The simultaneous increase of the Mg/Ca ratio with δ^{13}C indicates, as shown in Fig. 9(a), can be explained by three processes:

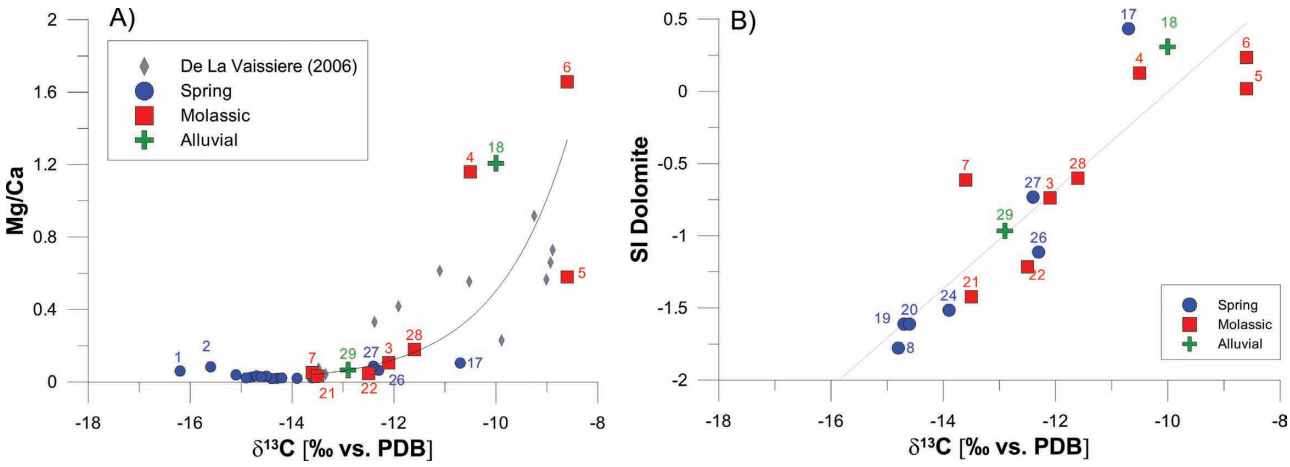

Figure 9. (a) Mg/Ca versus $\delta^{13}C$ and (b) Dolomite saturation index versus $\delta^{13}C$.

(1) A recrystallization or incongruent dissolution (concurrent dissolution and precipitation) of magnesian calcite[36] leading to a preferential partitioning of Mg and Sr into the liquid phase.
(2) The incongruent dissolution of dolomite leading to precipitation of calcite and a dedolomitization of the solid carbonates;
(3) The loss of Ca through cation exchange.

Indeed Fig. 9(b) shows the good correlation ($r^2 = 0.81$) between the isotopic composition and the saturation index with respect to dolomite. All these processes would lead to undersaturation with respect to calcite opening the possibility of supplementary carbonate dissolution. The increasing of $\delta^{13}C$ may be the result of such a renewed dissolution and the increase of Mg/Ca ratios is also compatible with the three reaction paths.

Concerning the first mechanism, a calcitic cementation of the molasse aquifer has been observed by de la Vaissière,[28] which is potentially due to a partial dissolution of the carbonate aquifer material and subsequent precipitation of ^{13}C-enriched calcite. According to the same author, cation exchange reactions are very limited in the regional aquifer system.

Initially, calcite will dissolve until calcite saturation is reached. Subsequent congruent or incongruent dolomite dissolution would be slower by an order of magnitude[53] and may add supplementary ^{13}C-enriched carbon to DIC, accompanied by an increase of Mg^{2+} in the liquid phase till equilibrium with respect to both calcite and dolomite is reached. The slow kinetics of such processes[36] might point to higher groundwater ages for the Mg-rich groundwaters.

Strontium isotopes approach

Strontium isotopes have been used for understanding water circulation in groundwater bodies, quantifying mixing of waters from different origins and examining geochemical interaction between water and aquifer rocks.[54–58] Moreover, major elements, mineral saturation state, and Sr/Ca versus $^{87}Sr/^{86}Sr$ help identifying the reactions that control the evolution of the waters chemistry, like the presence of incongruent dissolution of dolomites and calcite precipitation.[57]

A supplementary argument for ongoing incongruent dissolution for a subset of points are the Sr/Ca ratios combined with $^{87}Sr/^{86}Sr$ ratios (Fig. 10). Most waters show an evolution of $^{87}Sr/^{86}Sr$ ratios at near-constant Sr/Ca (arrow 2 in Fig. 10), indicating congruent dissolution of at least two types of carbonates with different isotopic composition but similar Sr/Ca. The high $^{87}Sr/^{86}Sr$ –low Sr/Ca end member is represented by springs #1 and 2 also characterized by low Mg/Ca and the lowest $\delta^{13}C$ and undersaturation with respect to calcite and dolomite. Both waters are the least evolved in terms of CO_2–water-carbonate interaction. The bulk of our groundwater samples show typical marine carbonate values at a fairly constant Sr/Ca ratio. Four wells # 18, 4 to 6 fall clearly off the general trend with high Sr/Ca and high $^{87}Sr/^{86}Sr$ (0.7087 to 0.7096). This may be explained (i) a third Sr-and Mg-rich carbonate end member in the system or (ii) incongruent dissolution of the less radiogenic end

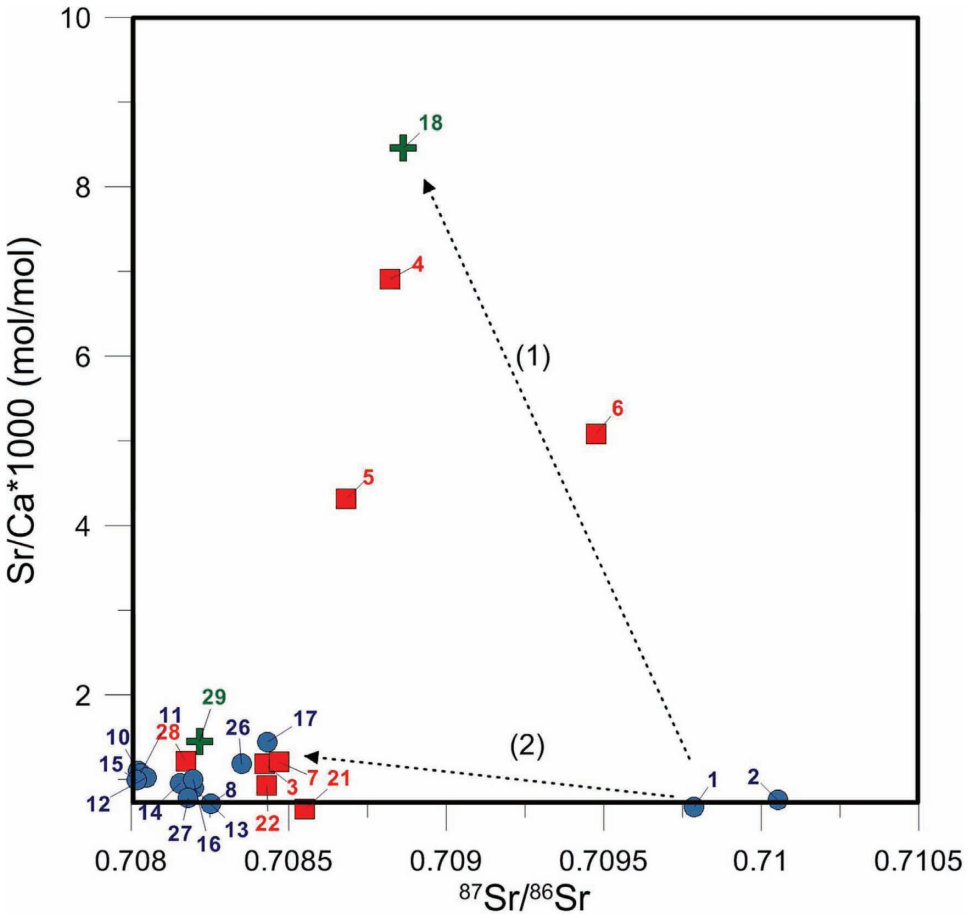

Figure 10. Evolution of Sr/Ca ratio versus $^{87}Sr/^{86}Sr$

member leading to preferential Sr partitioning into the liquid phase.

We can conclude that the $\delta^{13}C$ data for all samples combined with cation ratios and strontium isotope data can be explained by congruent and incongruent carbonate dissolution after equilibration with biogenic CO_2. There is no evidence of leakage of deep CO_2 into the shallow aquifer.

Conclusions

The zone of potential impact above the deep Montmiral CO_2 reservoir does not show any conclusive and unambiguous sign of deep CO_2 leakage. Waters of the shallow groundwater in the alluvial and molassic sediments are chemically rather homogenous except for some waters polluted by agricultural activities and a small subset of points with much higher Mg/Ca and Sr/Ca values. These waters are also the most enriched in ^{13}C so that mixing with deep-seated isotopically heavy CO_2 could be suspected. Water-rock interaction is obviously dominated by the evolution of the carbonate system even if relative sodium enrichment could point to minor cation exchange reaction with clays for some points. The forward modeling of the carbonate system for biogenic or geogenic CO_2 shows that the bulk of the measured groundwaters is compatible with carbonate dissolution by water in contact with a biogenic CO_2 soil reservoir. The enrichment in ^{13}C can be explained by incongruent Mg-calcite or dolomite dissolution without needing to consider mixing with deep geogenic CO_2. The latter mechanism could indeed be expected to isotopically enrich DIC but would rather enhance congruent dissolution without changes in the cation ratios. Lack of interaction with gaseous CO_2 of deep origin is also confirmed by the absence of a significant $\delta^{18}O$ shift toward more negative values as observed for example in the CO_2–rich fluids of the neighboring Central Massif.[40] To conclude, heavy deep CO_2 is not required

to explain the observed chemical and isotope data. Hence there is no sign of CO_2 leakage into shallow groundwater, which is consistent with the fact that the reservoir and caprock have been trapping the CO_2 efficiently over millions of years.

Acknowledgments

This study has been carried out in the framework of the RISCS project, co-funded by the EC 7th Framework Programme (FP7/2007-2013) under grant agreement no.240837 and by industrial partners ENEL I&I, Statoil, Vattenfall AB, E.ON and RWE. R&D partners are BGS, CERTH, IMARES, OGS, PML, SINTEF, University of Nottingham, Sapienza Università di Roma, Quintessa, CO_2GeoNet, Bioforsk, BGR, BRGM, NIVA and ZERO. Four R&D institutes outside Europe participate in RISCS: CO_2CRC from Australia, University of Regina from Canada and Montana State and Stanford Universities from the USA.

References

1. IEA Greenhouse Gas R&D Programme (IEA GHG), *Potential Impacts on Groundwater Resources of CO2 Storage,* Technical Study, Report 2011/11, IEA, Paris, France (2011).
2. Lions J, Devau N, De Lary L, Dupraz S, Gombert P, Dictor MC *et al.,* State of the art of the potential impacts of CO_2 geological storage leakage on fresh groundwater quality. *Int J Greenhouse Gas Control,* in press (2013).
3. André L, Audigane P, Azaroual M and Menjoz A, Numerical modeling of fluid-rock chemical interactions at the supercritical CO_2-liquid interface during CO_2 injection into a carbonate reservoir, the Dogger aquifer (Paris Basin, France). *Energ Convers Manage* **48**:1782–1797 (2007).
4. Kharaka Y, Thordsen J, Kakouros E, Ambats G, Herkelrath W, Beers S *et al.,* Changes in the chemistry of shallow groundwater related to the 2008 injection of CO_2 at the ZERT field site, Bozeman, Montana. *Environ Earth Sci* **60**(2):273–284 (2010).
5. Matter JM, Takahashi T and Goldberg D, Experimental evaluation of in situ CO_2-water-rock reactions during CO_2 injection in basaltic rocks: Implications for geological CO_2 sequestration, *Geochem Geophys Geosyst* **8**(2):Q02001 (2007)
6. Shevalier M, Nightingale M, Mayer B, Hutcheon I, Durocher K and Perkins E, Brine geochemistry changes induced by CO_2 injection observed over a 10 year period in the Weyburn oil field. *Int J Greenhouse Gas Control* **16**(1):S160–S176 (2013).
7. Audigane P, Gaus I, Czernichowski-Lauriol I, Pruess K and Xu T, Two-dimensional reactive transport modeling of CO_2 injection in a saline aquifer at the Sleipner site, North Sea. *Am J Sci* **307**(7):974–1008 (2007).
8. Audigane P, Lions J, Gaus I, Robelin C, Durst P, Van der Meer B, Geel K, Oldenburg C, Geochemical Modeling of CO_2 Injection into a Methane Gas Reservoir at the K12-B Field, North Sea, in *Carbon dioxide sequestration in geological media- State of the Science, AAPG Studies in Geology 59*, ed. by Grobe M, Paschin JC and Dodge RL, AAPG, Tulsa, Oklahoma, pp. 499–519 (2009).
9. Nicot JP, Evaluation of large-scale CO_2 storage on fresh-water sections of aquifers: An example from the Texas Gulf Coast Basin. *Int J Greenhouse Gas Control* **2(4):**582–593 (2008).
10. Yamamoto H, Zhang K, Karasaki K, Marui A, Uehara H and Nishikawa N, Numerical investigation concerning the impact of CO_2 geologic storage on regional groundwater flow. *Int J Greenhouse Gas Control* **3**(5):586–599 (2009).
11. Johnson G and Mayer B, Oxygen isotope exchange between H2O and CO_2 at elevated CO_2 pressures: Implications for monitoring of geological CO_2 storage. *Appl Geochem* **26**(7):1184–1191 (2011).
12. Johnson G, Mayer B, Nightingale M, Shevalier M and Hutcheon I, Using oxygen isotope ratios to quantitatively assess trapping mechanisms during CO_2 injection into geological reservoirs: The Pembina case study. *Chem Geol* **283**:185–193 (2011).
13. Mayer B, Shevalier M, Nightingale M, Kwon J-S, Johnson G, Raistrick M *et al.,* Tracing the movement and the fate of injected CO_2 at the IEA GHG Weyburn-Midale CO_2 Monitoring and Storage project (Saskatchewan, Canada) using carbon isotope ratios. *Int J Greenhouse Gas Control* **16**(1):S177–S184 (2013).
14. Quattrocchi F, Barbieri M, Bencini R, Cinti D, Durocher K, Galli G *et al.,* Strontium isotope (87SR/86SR) chemistry in produced oilfield waters: The IEA Weyburn CO_2 monitoring and storage project, in *Greenhouse Gas Control Technologies 7*, ed by Rubin ES, Keith DW, Gilboy CF, Wilson M, Morris T, Gale J *et al.* Elsevier Science Ltd, Oxford. pp. 2111–2114 (2005).
15. Myrttinen A, Becker V, van Geldern R, Würdemann H, Morozova D, Zimmer M *et al.,* Carbon and oxygen isotope indications for CO_2 behaviour after injection: First results from the Ketzin site (Germany). *Int J Greenhouse Gas Control* **4**(6):1000–1006 (2010).
16. Lewicki JL, Birkholzer J and Tsang CF, Natural and industrial analogues for leakage of CO_2 from storage reservoirs: Identification of features, events, and processes, and lessons learned. *Environ Geol* **52**:457–467 (2007).
17. Mörner NA and Ethiope G, Carbon degassing from the lithosphere. *Global Planet Change* **33**:185–203 (2002).
18. IEA Greenhouse Gas R&D Programme (IEA GHG), *Natural Releases of CO_2*, Report: 2005/08, IEA, Paris, France (2005).
19. Czernichowski-Lauriol I, Pauwels H, Vigouroux P and Le Nindre YM, The French Carbogaseous Province: An illustration of natural processes of CO_2 generation, migration, accumulation and leakage. *Greenhouse Gas Control Technologies - 6th International Conference.* Pergamon, Oxford (2003).
20. Keating E, Fessenden J, Kanjorski N, Koning D and Pawar R, The impact of CO_2 on shallow groundwater chemistry: Observations at a natural analog site and implications for carbon sequestration. *Environ Earth Sci* **60**(3):521–536 (2010).
21. IEA Greenhouse Gas R&D Programme (IEA GHG). *Caprock Systems for CO_2 Geological Storage*, Report: 2011/01, IEA, Paris, France (2011).
22. Beaubien SE, Ciotoli G, Coombs P, Dictor MC, Kruger M, Lombardi S *et al.,* The impact of naturally occurring CO_2 gas vent on the shallow ecosystem and soil chemistry of a Mediterranean pasture (Latera, Italy). *Int J Greenhouse Gas Control* **2:**373–387 (2008).
23. Gaus I, Le Guern C, Pearce J, Pauwels H, Shepherd T, Hatziynnis G *et al.,* Comparison of long-term geochemical

interactions at two natural CO_2-analogues: Montmiral (South-east Basin, France) and Messokampos (Florina Basin, Greece) case studies, in *Greenhouse Gas Control Technologies 7*, ed by Rubin ES, Keith DW, Gilboy CF, Wilson M, Morris T, Gale J *et al*. Elsevier Science Ltd, Oxford, pp. 561–569 (2005).

24. Pauwels H, Gaus I, le Nindre YM, Pearce J and Czernichowski-Lauriol I, Chemistry of fluids from a natural analogue for a geological CO_2 storage site (Montmiral, France): Lessons for CO_2–water–rock interaction assessment and monitoring. *Appl Geochem* **22**(12):2817–2833 (2007).
25. Humez P, Lagneau V, Lions J and Negrel P, Assessing the potential consequences of CO_2 leakage to freshwater resources: A batch-reaction experiment towards an isotopic tracing tool. *Appl Geochem* **30:**178–190 (2013).
26. Deines P, Langmuir D and Harmon RS, Stable isotope ratios and the existence of a gas phase in the evolution of carbonate groundwaters. *Geochim Cosmochim Acta* **38**:1147–1164 (1974).
27. Blavoux B and Dazy J, Caractérisation d'une province à CO_2 dans le bassin sud-Est de la France. *Hydrogéologie* **4**:241–252 (1990).
28. De la Vaissière R, *Etude de l'aquifère néogène du Bas-Dauphiné*, pHD. Université d'Avignon, France (2006).
29. Gal F, Le Pierres K, Brach M, Braibant G, Beny C, Battani A *et al.,* Surface gas geochemistry above the natural CO_2 reservoir of Montmiral (Drôme, France), source tracking and gas exchange between the soil, biosphere and atmosphere. *Oil Gas Sci Technol – Rev IFP* **65**(4):635–652 (2010).
30. Lafortune S, Moreira M, Agrinier P, Bonneville A, Schneider H and Catalette H, Noble gases as tools for subsurface monitoring of CO_2 leakage. *Energ Procedia* **1**(1):2185–2192 (2009).
31. Epstein S and Mayeda T, Variation of O18 content of waters from natural sources. *Geochim Cosmochim Acta* **4**:213–224 (1953).
32. Oshumi T and Fujini H, Isotope exchange technique for preparation of hydrogen gas in mass spectrometric D/H analysis of natural waters. *Anal Sci* **2**:489–490 (1986).
33. Pin C and Bassin C, Evaluation of a strontium specific extraction chromatographic method for isotopic analysis in geological materials. *Anal Chim Acta* **269**:249–255 (1992).
34. Celle-Jeanton H, Travi Y, Loÿe-Pilot MD, Huneau F and Bertrand G, Rainwater chemistry at a Mediterranean inland station (Avignon, France): Local contribution versus long-range supply. *Atmos Res* **91**:118–126 (2009).
35. Huneau F, *Fonctionnement hydrogéologique et archives paléoclimatiques d'un aquifère profond méditerranéen*, thèse de doctorat. Université d'Avignon et des Pays de Vaucluse, Avignon, France, pp. 192 (2000).
36. Edmunds WM, Cook JM, Darling WG, Kinniburgh DG, Miles DL, Bath AH *et al.,* Baseline geochemical conditions in the Chalk Aquifer, Berkshire, U.K.: A basis for groundwater quality management. *Appl Geochem* **2**:251–274 (1987).
37. Kloppmann W, Dever L and Edmunds WM, Residence time of Chalk groundwaters in the Paris Basin and the North German Basin: a geochemical approach. *Appl Geochem* **13:**593–606 (1998).
38. Blavoux B and Berthier F, Les originalités hydrogéologique et technique des eaux minérales. *Bull Soc Géol* **8**(1/7):1033–1044 (1985).
39. Celle H, Daniel M, Mudry J and Blavoux B, Signal pluie et traçage par les isotopes stables en Méditerranée occidentale. Exemple de la région avignonnaise (SE de la France). *C R Acad Sci Paris, Sciences de la Terre et des Planètes* **331:**647–650 (2000).
40. Pauwels H, Fouillac C, Goff F and Vuataz FD, Chemical and isotope geochemistry of CO_2 - rich thermal waters in the Mont Dore Massif, Massif Central, France. *Appl Geochem* **12**:411–427 (1997).
41. Casanova J, Bodénan F, Négrel P and Azaroual M, Microbial control on the precipitation of modern ferrihydrite and carbonate deposits from the Cézallier hydrothermal springs (Massif Central, France). *Sediment Geol* **126**:125–145 (1999).
42. Négrel Ph, Petelet-Giraud E, Serra H, Millot R and Kloppmann W, Caractéristiques hydrogéochimiques et isotopiques d'eaux thermo-minérales du Massif Central, in *Inventaire du potentiel géothermique de la Limagne (projet COPGEN),* BRGM/RP-53597-FR. pp. 173 (2004).
43. Johnson G, Raistrick M, Mayer B, Taylor S, Shevalier M, Nightingale M and Hutcheon I, The use of stable isotope measurements for monitoring and verification of CO_2 storage. *Energ Procedia* **1**(1):2315–2322 (2009).
44. Johnson G, Mayer B, Nightingale M, Shevalier M and Hutcheon I, Using oxygen isotope ratios to quantitatively assess trapping mechanisms during CO_2 injection into geological reservoirs: The Pembina case study. *Chem Geol* **283**:185–193 (2011).
45. Bottinga Y, Calculation of fractionation factors for carbon and oxygen isotopic exchange in the system calcite-carbon dioxide-water. *J Phys Chem* **72:**800–808 (1968).
46. Apps JA, Zheng L, Zhang Y, Xu T and Birkholzer JT, Evaluation of potential changes in groundwater quality in response to CO_2 leakage from deep geologic storage. *Transport Porous Med* **82**:215–246 (2010).
47. Lu J, Partin J, Hovorka S and Wong C, Potential risks to freshwater resources as a result of leakage from CO_2 geological storage: A batch-reaction experiment. *Environ Earth Sci* **60**(2):335–348 (2010).
48. Kharaka YK, Thordsen JJ, Hovorka SD, Seay Nance H, Cole DR, Phelps TJ *et al.,* Potential environmental issues of CO_2 storage in deep saline aquifers: Geochemical results from the Frio-I Brine Pilot test, Texas, USA. *Appl Geochem* **24**(6):1106–1112 (2009).
49. Parkhurst DL and Appelo CAJ, User's guide to PHREEQC (version 2) - A computer program for speciation, reaction-path, 1D-transport, and inverse geochemical calculations, in *US Geological Survey Water Resource Investigations Report 99-4259*, Denver, Colorado, pp. 312 (1999).
50. Blanc P, Lassin A and Piantone P, *THERMODDEM a database devoted to waste minerals*. [Online]. BRGM (Orléans, France) (2007). Available at: http://thermoddem.brgm.fr [15 December 2011].
51. Mook WG, Carbon-14 in hydrogeological studies, in *Handbook of Environmental Isotope Geochemistry*, Vol. 1, ed. by P. Fritz and J. C. Fontes. Elsevier, New York, pp. 49–74 (1980).
52. Wigley TML, Carbon-14 dating of groundwater from closed to open systems. *Water Resour Res* **11**:324–328 (1975).
53. Pokrovsky O S, Golubev S V, Schott J and Castillo A, Calcite, dolomite and magnesite dissolution kinetics in aqueous solutions at acid to circum neutral pH, 25 to 150°C and 1 to 55 atm pCO_2: New constraints on CO_2 sequestration in sedimentary basins. *Chem Geol* **265**:20–33 (2009).
54. Jacobson AD and Wasserburg G J, Anhydrite and the Sr isotope evolution of groundwater in a carbonate aquifer. *Chem Geol* **214**(3/4):331–350 (2005).
55. Katz BG, Catches JS, Bullen TD and Michel RL, Changes in the isotopic and chemical composition of ground water

resulting from a recharge pulse from a sinking stream. *J Hydrol* **211**(1/4):178–207 (1998).

56. Kloppmann WP, Négrel Ph, Casanova J, Klinge H, Schelkes K and Guerrot C, Halite dissolution derived brines in the vicinity of a Permian salt dome (N German Basin). Evidence from boron, strontium, oxygen, and hydrogen isotopes. *Geochim Cosmochim Acta* **65**(22):4087–4101 (2001).
57. Oetting GC, Banner JL and Sharp JM, Regional controls on the geochemical evolution of saline groundwaters in the Edwards aquifer, central Texas. *J Hydrol* **181**(1/4):251–283 (1996).
58. Petelet E, Luck JM, Ben Othman D, Negrel P and Aquilina L, Geochemistry and water dynamics of a medium-sized watershed: The Hérault, southern France: 1. Organisation of the different water reservoirs as constrained by Sr isotopes, major, and trace elements. *Chem Geol* **150**(1/2):63–83 (1998).

Julie Lions

Julie Lions is hydrogeochemist working for the Water Environment & Ecotechnologies Division, BRGM (France) since 2005. She obtained a PhD in inorganic pollutant mobility in vadose zone and groundwater (2004). She's currently involved in several projects on potential impacts of leakages from CO_2 geological storage into fresh groundwater.

Pauline Humez

Pauline Humez holds a PhD in isotope hydrogeochemistry from Ecole des Mines ParisTech and BRGM. Research interests are gas-water-rock interaction, multi-isotope tracing, reactive transport modeling, she is now in Applied Geochemistry Group in the Department of Geoscience (University of Calgary) for a Postdoctoral position.

Hélène Pauwels

Hélène Pauwels is currently a senior scientist and project manager with more than 20 years with the BRGM (French geological Survey). Her expertise lies in water quality, especially relating to groundwater and water-rock interactions.

Wolfram Kloppmann

Wolfram Kloppmann helds a PhD in isotope hydrogeochemistry from Paris XI University (France). Working in the fields of chemistry and isotope characteristics of natural fluids, water-rock interaction, and environmental issues related to groundwater quality and non-conventional water resources, he is in charge of the BRGM isotope laboratory.

Isabelle Czernichowski-Lauriol

Isabelle Czernichowski-Lauriol has a PhD in Geosciences. Since 1993, she has played a leading role in pioneering research programmes on CO_2 geological storage. She is currently President of the CO2GeoNet Association, Programme Officer on Geo-Energy at the Direction of Research of BRGM and CCS Programme Officer at the French National Research Agency.

